



A DEMS approach for the direct detection of CO formed during electrochemical CO₂ reduction

Christoph J. Bondue, Marc T.M. Koper*

Leiden Institute of Chemistry, Leiden University, P.O. Box 9502, 2300, RA, Leiden, the Netherlands

ARTICLE INFO

Article history:

Received 2 October 2019

Received in revised form 7 January 2020

Accepted 9 January 2020

Available online 11 January 2020

Keywords:

CO₂ reduction reaction

DEMS

CO-detection

Flow cell

Mass spectroscopy

ABSTRACT

Observation of CO formed during electrochemical CO₂ reduction using Differential Electrochemical Mass Spectrometry (DEMS) is complicated by the fragmentation of CO₂ in the course of the ionization process. Since much more CO₂ than CO enters the vacuum of the mass spectrometer, the ion current for mass 28 is dominated by the CO⁺-fragment of CO₂. By reducing the cathode potential of the ion source of the mass spectrometer from -70 V to -27.5 V, fragmentation of CO₂ is reduced to a negligible degree. This allows direct observation of electrochemically formed CO by measuring the ionic current for mass 28. We show that this method is superior to matrix calibration in which the ionic current for mass 44 corrected by the CO⁺/CO₂⁺-intensity ratio is subtracted from the ionic current for mass 28. Using this method, we compare DEMS results for the electrochemical reduction of CO₂ at gold electrodes obtained in two different cells, a conventional DEMS cell with the working electrode sputtered onto the membrane in contact with the vacuum and a flow cell where the interface to the vacuum is separated from the working electrode. We show that in the conventional cell at the interface between electrolyte and vacuum, the local CO₂ concentration is reduced as the nearby vacuum interferes with the equilibria of reactions involving gases, and the local pH is increased. Therefore, in DEMS cells where the working electrode is positioned in the vicinity of the interface, the onset potential for CO₂ reduction and hydrogen evolution are shifted and the observed faradaic efficiency for CO₂ reduction are considerably reduced compared to literature values. This can be rectified by using flow cells that allow a spatial separation between vacuum/electrolyte interface and working electrode. We describe how the Dual Thin Layer Cell can be calibrated for detecting CO, thus allowing quantification of evolved amounts of CO from the ionic current for mass 28.

© 2020 The Authors. Published by Elsevier B.V. This is an open access article under the CC BY license (<http://creativecommons.org/licenses/by/4.0/>).

1. Introduction

Electrochemical Mass Spectrometry (EMS) was introduced by Bruckenstein and Gadde [1] and provides the means to detect (volatile) products of electrochemical reactions via mass spectroscopy. In their original setup, Bruckenstein and Gadde first collected volatile reaction products through a hydrophobic membrane into a vacuum system for approximately 20 s and then released them for detection into the vacuum of the mass spectrometer [1,2]. Their setup allowed, for the first time, the quantitative and in situ detection of volatile reaction products. Although this approach was able to correlate the faradaic charge in the electrochemical cell to the ionic charge in the mass spectrometer, the same could not be achieved for the respective currents.

In the 1980s, EMS was improved by Wolter and Heitbaum to allow the correlation of faradaic and ionic current [3]. As the current is the differential of the charge, the technique introduced by Wolter and

Heitbaum was called differential electrochemical mass spectroscopy (DEMS) [3]. This was achieved by creating a differentially pumped vacuum system in which the ion source of the mass spectrometer resided at a higher pressure than the detector [3]. In this design, the electrochemical cell is attached directly to the vacuum of the mass spectrometer, which makes it possible to collect volatile reaction products continuously. A porous hydrophobic Teflon membrane forms the interface between vacuum and electrolyte. Since Wolter and Heitbaum deposited the working electrode on the membrane, volatile reaction products are formed in the vicinity of the interface between vacuum and electrolyte [3]. Therefore volatile reaction products can reach the mass spectrometer with a short time constant.

Although limited to volatile reaction products (but see ref.: [4]), DEMS has become a powerful tool to elucidate the mechanism of hydrogenation reactions [5], the oxidation of alcohols [6–8] or the working principle of metal oxide catalysts [9]. Recently DEMS has also proven its usefulness for the electrochemical reduction of CO₂ as it allows the online, quantitative detection of a large variety of volatile compounds in parallel [10–12]. However, detection of CO in the course of CO₂-

* Corresponding author.

E-mail address: m.koper@chem.leidenuniv.nl (M.T.M. Koper).

reduction is still difficult. Due to the equilibrium between CO₂ and bicarbonate, there is always CO₂ in the vicinity of the vacuum/electrolyte interface that constantly evaporates into the vacuum of the mass spectrometer. However, the amount of CO₂ entering the mass spectrometer depends on the pH at the interface, which changes locally when hydrogen evolution proceeds parallel to CO₂ reduction. This will cause large shifts in the baseline of the ionic current for mass 44 (CO₂-molecular peak). In addition, due to the fragmentation of CO₂ to CO⁺ in the course of the ionization process, a high baseline in the ionic current for mass 28 is observed as well. This renders it at least difficult to detect reliably the evolution of CO. In previous papers, matrix calibration was chosen to separate the contributions from CO and CO₂ to the ionic current for mass 44 [11,13]. In this approach the ionic current for mass 44 multiplied with the fragmentation factor is subtracted from the ionic current for mass 28, thus yielding the signal due to CO evolution. The drawback of this approach is the high noise level of the CO₂ signal that is transferred to the extrapolated CO signal.

An alternative is to detect CO via gas chromatography (GC) [14]. With this approach the evolved gas mixture is collected and after a certain period separated chromatographically into its different components, which are detected and characterized by various means. This is reminiscent of the EMS approach, but due to its lower sensitivity GC-measurements usually require large sample volumes and therefore collection times longer than 20 s. For that reason GC-measurements are generally long and are unable to capture rapid changes of product distribution that often occur in the very beginning of the measurement due to poisoning or other fast transformations of the electrode surface.

In contrast to GC measurements, DEMS-cells in which the working electrode is placed immediately at the electrolyte/vacuum interface allow direct detection of electrochemically evolved volatile reaction products with a collection efficiency of close to 100% [2,3,15], which however decreases to lower values under increased mass transport conditions in the electrolyte [16]. Due to the high sensitivity of mass spectroscopy, even minor quantities, for instance the electrochemical desorption of submonolayers on single crystal surfaces, can be observed [17]. However, not only products of the electrochemical reaction evaporate at the vacuum/electrolyte interface but also the gaseous reactants thus depleting their concentrations in the vicinity of the working electrode [18]. For the specific case of CO₂ reduction, this means that the CO₂/bicarbonate equilibrium is shifted, which might affect the electrochemical reaction. This problem can be overcome by utilizing flow cells such as the Dual Thin Layer Cell in which working electrode and vacuum/electrolyte interface are separated [2,19].

In the present article we demonstrate (i) how the choice of the DEMS cell affects the results obtained for CO₂ reduction, and (ii) how DEMS can be used to detect directly the electrochemical formation of CO in the course of CO₂-reduction by adjusting the settings of the ion source. We are going to show that an unreasonably low faradaic efficiency for CO formation is measured when the working electrode is placed at the vacuum/electrolyte interface. This is attributed to the effect of the vacuum on local CO₂ concentration. By contrast, a faradaic efficiency close to the literature value is obtained when the dual thin layer cell is employed. By adjusting the settings of the ion source, fragmentation of CO₂ during ionization can be suppressed and direct observation of electrochemically formed CO via DEMS becomes possible.

2. Experimental

2.1. DEMS setup

The experiments presented in this article were conducted on a home-built DEMS system following the design principles outlined by Wolter and Heitbaum [3]. In our setup the mass spectrometer (Hiquad™ QMA 410, Pfeiffer Vacuum) is situated in a differentially pumped vacuum chamber. A sleeve manufactured from PEEK placed around the mass filter and with a short distance from the ion source separates the vacuum system into

two sections. The first section that volatile compounds enter from the electrochemical cell is kept at pressures below 5·10⁻² Pa by a turbomolecular pump with a pumping speed of 255 L/s (HiPace 300, Pfeiffer Vacuum). A smaller turbomolecular pump with a pumping speed of 66 L/s (HiPace80, Pfeiffer Vacuum) keeps the pressure in the second chamber below the operation limit of the secondary electron multiplier (SEM) of 10⁻³ Pa. The mass spectrometer features a crossbeam ion source and we choose yttriated iridium as material for the filament.

2.2. Leakage calibration

In order to determine the sensitivity of the DEMS-setup we conducted leakage calibration as outlined previously by Wolter and Heitbaum [3,15]. To that end we filled a known volume with the gas for which we sought calibration to a pressure lower than 600 Pa. In order to achieve a gas-type independent and highly accurate measurement of the pressure we choose a capacitive gauge (CMR 363, Pfeiffer Vacuum) and recorded the pressure in the volume as a function of time (PVActiveLine, Pfeiffer Vacuum). Through a dosing valve (EVN 116, Pfeiffer Vacuum) the gas was expanded into the vacuum of the mass spectrometer, while recording the ionic current for the relevant masses in “Multiple Ion Detection Mode” as a function of time.

The decline of the measured pressure corresponds to the amount of gas molecules leaking from the volume into the vacuum of the mass spectrometer. Applying the gas equation and deriving with respect to time yields the flow of gas molecules in mol/s, which decreases over time as the pressure in the volume decreases. Plotting the measured ion current as a function of the flux yields a straight line the slope of which gives the sensitivity of the mass spectrometer in C/mol. In order to avoid errors due to non-linearity in partial pressure measurements we calibrated under conditions as in the measurement (i.e. with the electrochemical cell attached) and adjusted the flux to a range similar as expected for electrochemically generated molecules.

2.3. Electrochemical measurements and cells

For measurements with the electrode sputtered onto the Teflon membrane the “classical” or “conventional” cell was used. The cell was described previously by Baltruschat [2]. In this cell setup, a gold film of 50 nm thickness sputtered on a porous Teflon membrane is used as the working electrode. For mechanical support a steel frit is placed on the vacuum side underneath the membrane. On the other side the electrolyte rests on the membrane in contact with the gold film. Hence, the electrochemical reactions take place at the interface between electrolyte and vacuum.

The Dual Thin Layer Cell introduced by Jusys and Baltruschat [19] and described in detail elsewhere [2] was used for those measurements where the electrode was separated from the vacuum electrolyte interface. The flow through the Dual Thin Layer Cell was adjusted by a syringe pump (NE1600, ProSense), which pumped the electrolyte from a storage container through the cell.

The reference electrode used for this study was a hydrogen electrode in a phosphate buffered electrolyte (0.05 M NaH₂PO₄ and 0.05 M Na₂HPO₄). A schematic drawing of how the DEMS cell and reference electrode are combined can be found elsewhere [20]. Gold wires where used as counter electrodes. NaClO₄ and NaCO₃ were purchased from Sigma Aldrich. The Teflon membrane (Emflon, Pall Cooperation, Lot Number: 139403) used to create the interface between electrolyte and vacuum had a pore size of 15 nm. The Membrane was removed mechanically from the support.

2.4. Quantification of the ionic current

The following equations are used to determine the partial faradaic current (subscript “F”) due to the formation of any species x from the ionic current for mass m:

$$I_{\text{ion},x}(m) = n_{\text{F},x} K_x^{\ominus}(m) = n_{\text{F},x} N_x K_x^{\oplus}(m)$$

$$I_{\text{ion},x}(m) = \frac{I_{F,x}}{z_x \cdot F} \cdot N_x \cdot K_x^*(m) \quad (1b)$$

In Eq. (1a), the ionic current (subscript “ion”) for mass m and for a given species x ($I_{\text{ion},x}(m)$) is proportional to the amount of species x formed electrochemically per unit of time ($\dot{n}_{F,x}$). The proportionality constant in Eq. (1a) is K_x^* and is the product of two factors, N_x and $K_x^*(m)$ [2]. N_x is the transfer efficiency of the cell and gives the fraction of electrochemically formed species x that enters the vacuum of the mass spectrometer [2]. $K_x^*(m)$ is the sensitivity of the mass spectrometric setup to detect species x in the ionic current for mass m . A number of factors, in particular pumping speed, fragmentation pattern of species x , the settings and state of the ion source, enter into $K_x^*(m)$ [2]. Particularly under the operation conditions of our DEMS setup the state of the ion source constantly changes and $K_x^*(m)$ must be measured for each experiment and for each species individually. After applying Faraday's law, $\dot{n}_{F,x}$ can be replaced in Eq. (1b) by the partial faradaic current for the formation of species x $I_{F,x}$ divided by Faraday's constant and the number of electrons transferred during the formation of one molecule of species x (z_x).

For the classical cell we can assume that the transfer efficiency is close to 100%, i.e. $N_x = 1$ [3,15].

2.5. Calibration of the dual thin layer cell

For the Dual Thin Layer Cell we cannot assume that N_x is 100% [2], hence quantification of the ionic currents measured with this cell requires a calibration method to determine either N_x or $K_x^*(m)$. Since N_x is related to the concentration profile of species x in the electrolyte [2], it is affected by both electrolyte flow rate and diffusion coefficient of species x . Furthermore, N_x is affected by the exact geometry of the cell setup that cannot be reproduced reliably after disassembling the cell. Hence, calibration has to be conducted for each flow rate, for each species and for each cell setup. The discussion in the Supporting Information provides a detailed explanation why these factors enter the transfer efficiency.

Calibration of the cell can be achieved relatively easy for hydrogen and oxygen: In the absence of bicarbonate, that is, in the blank electrolyte of 0.9 M NaClO₄ hydrogen evolution proceeds with a faradaic efficiency of 100%. After conducting this type of experiment we were able to determine $K_{\text{H}_2}^*(2)$ from the faradaic charge and the ionic charge for mass 2 measured in the potential region of hydrogen evolution [2]. Without disassembling the cell it is possible to switch the electrolyte to an aqueous solution of 0.1 M NaHCO₃ in 0.9 M NaClO₄. Oxygen evolution is not affected by the presence of bicarbonate and proceeds with a faradaic efficiency of 100%. Hence, $K_{\text{O}_2}^*(32)$ can be determined from the faradaic charge and the ionic charge for mass 32 in the potential region of oxygen evolution [2]. From $K_{\text{O}_2}^*(32)$, and from leakage calibration for oxygen yielding $K_{\text{O}_2}^*(32)$, we can determine N_{O_2} . The discussion in the Supporting Information provides a detailed explanation why calibration cannot be achieved by other means.

Since the diffusion coefficients for O₂ ($1.98 \cdot 10^{-5} \text{cm}^2/\text{s}$) [21] and CO ($2.03 \cdot 10^{-5} \text{cm}^2/\text{s}$) [22] are similar in water, we will assume that N_{CO} equals N_{O_2} . A similar assumption has been made before [23]. After leakage calibration for CO, we can determine $K_{\text{CO}}^*(28)$ from N_{CO} and $K_{\text{O}_2}^*(32)$.

Calibration for CO can also be achieved by the bulk oxidation of CO. $K_{\text{CO}}^*(28)$ is then obtained from the ionic current for mass 28, which will be negative after baseline correction, and from the faradaic current of the oxidation process. However, this method will only be quantitatively reliable if the current for CO oxidation on the same material is not convoluted by other Faradaic processes.

3. Results and discussion

Fig. 1 shows the results of a DEMS experiment conducted with the classical cell [2] employing a gold sputtered Teflon membrane as working electrode and an aqueous solution of 0.9 M NaClO₄ and 0.1 M NaHCO₃.

The faradaic current measured in the classical cell is displayed in Fig. 1A. As the potential passes -0.4 V in the negative going scan, a reduction process is observed. This is accompanied by the evolution of a signal in the ionic current for mass 2 (Fig. 1B), indicating the electrochemical formation of H₂. On the other hand an oxidation process at potentials larger 1.8 V is observed that is paralleled by a signal in the ionic current for mass 32, indicative for the electrochemical evolution of oxygen.

It is evident from the red curve in Fig. 1C that the ionic current for mass 44 decreases significantly (note the unit: μA) parallel to HER and increases as the potential region of oxygen evolution is entered. While the decreasing amount of CO₂ entering the mass spectrometer parallel to hydrogen evolution might be due to the electrochemical consumption of CO₂ in the course of CO formation, the increasing ionic current for mass 44 parallel to OER suggest that another effect is responsible for the observed signals. Given that HER and OER alter the local pH in the vicinity of the electrode it is necessary to consider the equilibrium between bicarbonate and CO₂ in Eq. (2):



In the course of hydrogen evolution OH⁻ is produced which shifts the equilibrium in Eq. (2) to the left side. Hence, in the vicinity of the interface between vacuum and electrolyte less CO₂ is present, and fewer CO₂ molecules enter the vacuum of the mass spectrometer. The opposite occurs during OER, where the lower local pH value increases the CO₂ concentration. The effect of the local pH on the ionic current for mass 44 renders it difficult to derive any information on the amount of electrochemically reduced CO₂.

The black curve in Fig. 1C shows the ionic current for mass 28 that we measured with a cathode potential of the ion source of the mass spectrometer set to -70 V. It follows the same trend as the ionic current for mass 44. This is due to the formation of an CO⁺-fragment during electron impacted ionization of CO₂. Because of the large amounts of CO₂ entering the vacuum

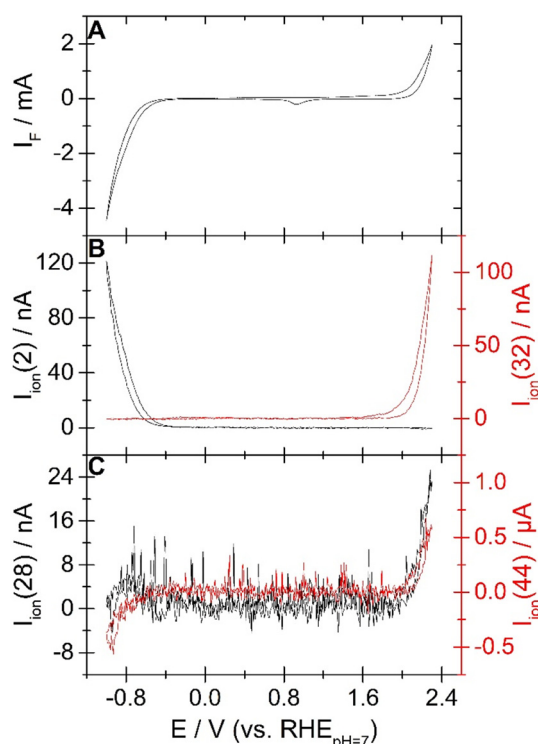


Fig. 1. DEMS experiment using the classical cell. The working electrode is a thin gold film (approximately 50 nm) sputter deposited on the Teflon membrane. The electrolyte is an aqueous solution of 0.9 M NaClO₄ and 0.1 M NaHCO₃ purged with CO₂. A: faradaic current; B: Ionic current for mass 2 (black curve, left y-scale) and for mass 32 (red curve, right y-scale); C: Ionic current for mass 28 (black curve, left y-scale) and for mass 44 (red curve, right y-scale). Cathode potential of ion source: -70 V. Sweep rate: 20 mV/s.

of the mass spectrometer, its CO^+ -fragment dominates the ionic current for mass 28. As a result, the ionic current for mass 28 is combined with the amount of evolved CO as well as with the pH-effect on the local CO_2 -concentration. It is therefore difficult to quantify the amount of CO formed in the course of CO_2 reduction via mass spectroscopy under these conditions. Previously, matrix calibration was performed in order to separate the contributions of CO and CO_2 from each other [11,13]. For the curves in Fig. 1 we can employ Eq. (3) to eliminate the contribution of CO_2 to the ionic current for mass 28.

$$I_{\text{ion}}^{\text{CO}}(28) = I_{\text{ion}}^{\text{tot}}(28) - f_{\text{ion}} \cdot I_{\text{ion}}(44) \quad (3)$$

In Eq. (3) $I_{\text{ion}}^{\text{tot}}(28)$ is the total measured ionic current for mass 28, $I_{\text{ion}}(44)$ is the measured ionic current for mass 44, $I_{\text{ion}}^{\text{CO}}(28)$ is the ionic current for mass 28 corrected for the contribution of CO_2 , and f_{ion} is the relative intensity of the 28 fragment of CO_2 as compared to the intensity of the 44-fragment. f_{ion} can be derived from experiments shown in Fig. 2B, showing the ionic currents for mass 44 and 28, respectively, during a leakage calibration experiment (see Experimental Section). These currents were measured while leaking CO_2 with the flow rate shown in Fig. 2A into the vacuum of the mass spectrometer. With a cathode potential of the ion source of -70 V, f_{ion} was determined to be 0.048.

Fig. 3B shows $I_{\text{ion}}^{\text{CO}}(28)$ after applying Eq. (3) to the ionic current for mass 28 and 44 shown in Fig. 1C. For better comparison Fig. 3A also features the faradaic current already shown in Fig. 1A. The evolution of a signal in the corrected ionic current for mass 28 indicates the formation of CO. After leakage calibration for CO, we employed Eq. (1b) to determine the partial faradaic current due to CO-formation from $I_{\text{ion}}^{\text{CO}}(28)$ in Fig. 3B. Dividing the partial faradaic current due to CO formation by the faradaic current yields the faradaic efficiency shown in Fig. 3C as a function of the applied potential. The 10% faradaic efficiency is quite low compared to values close to 100% observed in the literature [14]. Since the working electrode is located in the direct vicinity of the interface between vacuum and electrolyte, constant evaporation lowers the local CO_2 -concentration, resulting in the low faradaic efficiency for CO formation of 10%. Cells such as the

classical cell in which the working electrode is placed in the direct vicinity of the vacuum/electrolyte interface appear therefore unsuitable to investigate CO_2 reduction with DEMS. This observation that the classical DEMS setup disturbs chemical equilibria in solution involving volatile species, and may therefore distort measurement results, has been made before in a study of the reduction of nitrate of platinum electrodes [18].

Notwithstanding this drawback of the classical cell, matrix calibration appears to be a valid method to separate the CO_2 -contributions to the ionic current for mass 28 in order to obtain the signal due to CO formation. However, Fig. 3B also shows that the corrected ionic current for mass 28 features a rather high noise level, which arises from the high base line of the ionic current for mass 28 and from the high noise level of the ionic current for mass 44 that is transferred via Eq. (3) to $I_{\text{ion}}^{\text{CO}}(28)$. Furthermore, matrix calibration becomes increasingly complicated and prone to errors as more molecules can contribute to the ionic current for mass 44 (acetaldehyde) or the ionic current for mass 28 (ethanol, methanol, ethylene). In order to observe the evolution of CO in the course of CO_2 reduction via mass spectroscopy it would be desirable to measure the ionic current for mass 28 without any contribution from other molecules than CO.

Fig. 2D shows the ionic currents for mass 44 and 28, respectively, that were measured when CO_2 was leaked into the vacuum with the flow rate shown in Fig. 2C. In this measurement, the cathode potential of the ion source of the mass spectrometer was set to -27.5 V. With a less negative cathode potential the energy of the emitted electrons and therefore the energy of the electron impact during the ionization process is reduced. As a consequence the fragmentation of CO_2 becomes negligibly small as evidenced by the missing signal in the ionic current for mass 28 when CO_2 is introduced into the vacuum chamber.

Therefore, we conducted the same experiment as that in Fig. 1 but with the cathode potential of the ion source set to -27.5 V. This was done for better comparison, despite the observation that the classical cell appears to be unsuitable for the investigation of CO_2 reduction. The black curve in Fig. 4A shows the faradaic current measured during the experiment. Essentially the same observations as in Fig. 1 are made: At potentials lower -0.4 V a negative faradaic current and a positive ionic current for mass 2

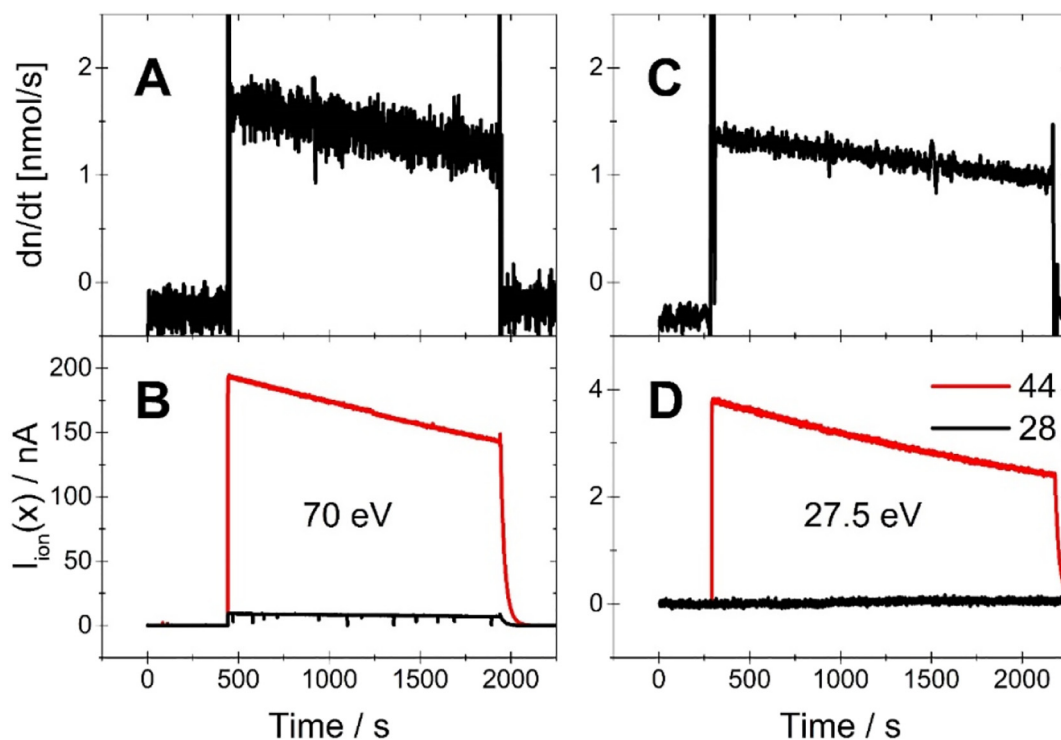


Fig. 2. Flow rate of CO_2 into the vacuum system of the mass spectrometer (A, C) and the ionic current for mass 44 (red) and 28 (black) as a function of time (B, D). The cathode potential of the ion source was -70 V (B) and -27.5 V (D), respectively. Note the different Y-scales for panel B and D.

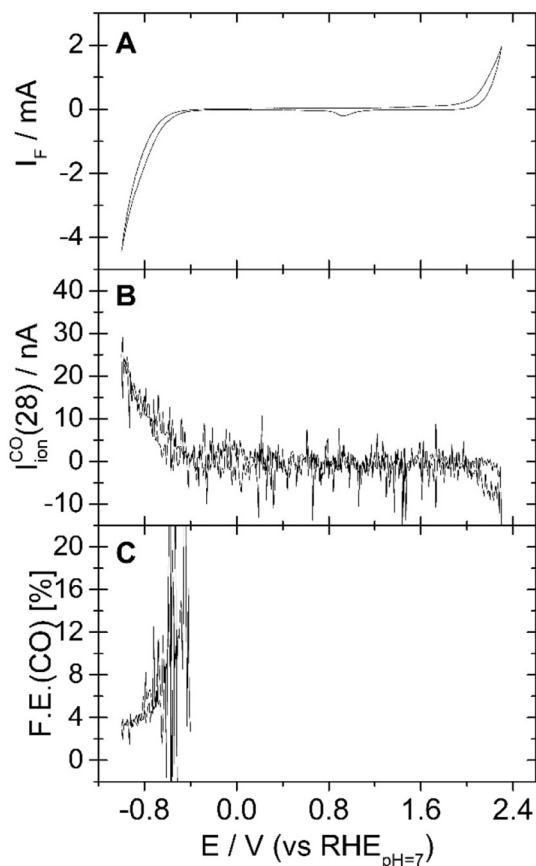


Fig. 3. Faradaic current as shown in Fig. 1A (A) and the ionic current for mass 28 (B) after correcting for the CO_2 signal via Eq. (3) taking into account the fragmentation pattern as determined from the curve in Fig. 2B. C: Faradaic efficiency for CO formation.

in Fig. 4B is observed. At potentials larger 1.8 V oxygen evolution takes place as signified by a positive faradaic current in Fig. 4A and a positive ionic current for mass 32 in Fig. 4B. The overall ionic current for mass 2 and mass 32 is lower than in Fig. 1B. This is due to the lower ionization probability during electron impact ionization when the energy of the electrons is reduced. However, a good signal-to-noise ratio is obtained nonetheless. Furthermore, the shape of the ionic currents follows the trend expected from the faradaic current and is not distorted. This shows that stable operation of the ion source is possible, when the cathode potential is set to -27.5 V.

Also the ionic current for mass 44 shows the same behavior as in Fig. 1C: parallel to oxygen evolution the ionic current for mass 44 increases and then decreases parallel to hydrogen evolution. However, different from Fig. 1C the ionic current for mass 28 does not follow this trend. Since fragmentation of CO_2 takes place to a negligible degree, the signal in the ionic current for mass 28 is only due to the electrochemical formation of CO. While there is no apparent disadvantage to the use of a lower cathode potential (provided the mass spectrometer allows these settings), a notable advantage is the much lower noise level as compared to the curve shown in Fig. 3B that was obtained via matrix calibration.

In the same way as for Fig. 3C, we determined the faradaic efficiency for CO formation from the ionic current for mass 28, as shown in Fig. 4D. The faradaic efficiency never exceeds 10% confirming that the vacuum changes the reaction conditions at the location of the working electrode as compared to experiments conducted under ambient conditions [14].

In order to avoid the effect of the nearby vacuum on CO_2 reduction in the classical DEMS cell, we employed the Dual Thin Layer Cell (c.f. Fig. S1 in the Supporting Information) introduced by Jusys and Baltruschat [2,19]. The cell consists of two compartments: one compartment in which the electrochemistry is conducted and another compartment in which the

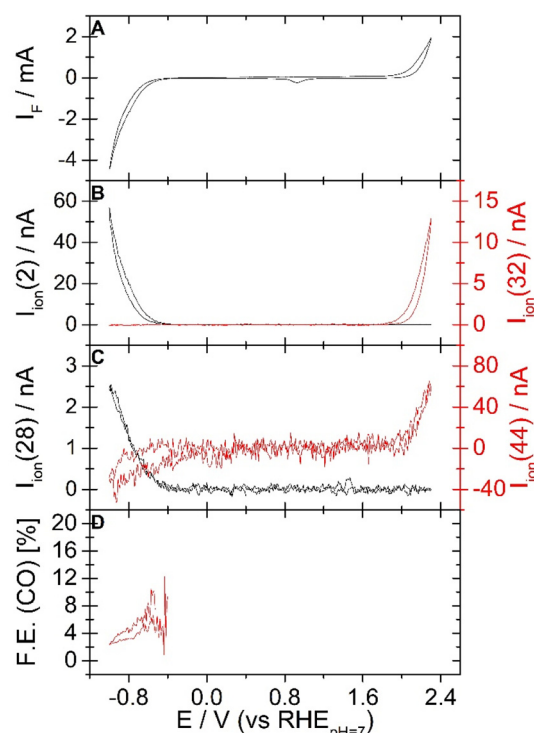


Fig. 4. DEMS experiment using the classical cell. The working electrode is a thin gold film (approximately 50 nm) sputter deposited on the Teflon membrane. The electrolyte is an aqueous solution of 0.9 M NaClO_4 and 0.1 M NaHCO_3 purged with CO_2 . A: measured faradaic current (black); B: Ionic current for mass 2 (black curve, left y-scale) and mass 32 (red curve, right y-scale); C: Ionic current for mass 28 (black curve, left y-scale) and mass 44 (red curve, right y-scale). D: Faradaic efficiency for CO formation as determined from the ionic current for mass 2 and 28. Cathode potential of ion source: -70 V. Sweep rate: 20 mV/s.

interface between electrolyte and vacuum is created. The compartments are connected with each other and a constant electrolyte flow transports the products of the electrochemical reaction from the first compartment to the second, where they can evaporate into the vacuum of the mass spectrometer.

Fig. 5A shows the faradaic current obtained at a massive, polycrystalline gold electrode. Parallel to the oxidation process observed in the CV, in Fig. 5B a signal evolves in the ionic current for mass 32 as the potential exceeds 1.9 V. Compared to the results obtained in the classical cell the onset potential for oxygen evolution is shifted by roughly 0.1 V to higher values. Also the onset potentials of the reduction process due to hydrogen evolution and CO_2 reduction, as evidenced by the signals in the ionic currents for mass 2 and 28 (Fig. 5C), are shifted positively by 0.1 V, as compared to the CVs obtained in the classical cell.

Following the procedure outlined in the experimental part, we determined $K_{\text{H}_2}^{\ominus}(2)$ and $K_{\text{CO}_2}^{\ominus}(28)$, which allows us to calculate the partial faradaic current due to hydrogen evolution and CO formation from the respective ionic currents. The sum of both currents is plotted as a function of potential in Fig. 5A. In the potential region lower than -0.3 V the measured faradaic current and the faradaic current predicted from the ionic current for mass 2 and 28 match each other quite well. This justifies retrospectively the assumption that N_{CO} equals N_{O_2} and validates the method used here to quantify the amounts of evolved CO and H_2 .

Fig. 5D shows the faradaic efficiency for CO formation, which was calculated from the partial current densities determined from the ionic currents for mass 2 and 28. At -0.5 V a faradaic efficiency of about 90% is achieved. The deviation from a faradaic efficiency of 100% reported in previous studies [14] might be due a different cell geometry with different mass transport conditions as well as to a lower detection limit for hydrogen than in our experimental setup.

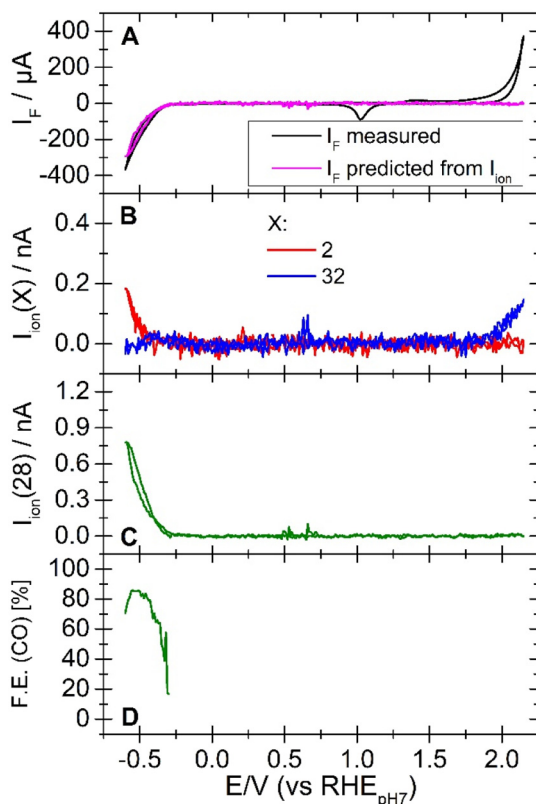


Fig. 5. DEMS experiment using the Dual Thin Layer Cell. The working electrode is a massive, polycrystalline gold. The electrolyte is an aqueous solution of 0.9 M NaClO₄ and 0.1 M NaHCO₃ purged with CO₂. A: measured faradaic current (black) and faradaic current determined from the ionic current for mass 2 and 28 (magenta); B: Ionic current for mass 2 (red) and mass 32 (blue); C: Ionic current for mass 28. D: Faradaic efficiency for CO formation as determined from the ionic current for mass 2 and 28. Cathode potential of ion source: -27.5 V. Sweep rate: 20 mV/s.

Irrespective of the exact value of the faradaic efficiency for CO₂ reduction, it is obvious that it is an order of magnitude higher than the value determined in the classical cell, and close to the literature value [14]. The deviation of the faradaic efficiencies for CO formation determined in the classical cell and the Dual Thin Layer affirms our conclusion that the vacuum affects quite significantly the bicarbonate/CO₂ equilibrium in the vicinity of the electrolyte/vacuum interface. Furthermore, the 0.1 V shift of the onset potential observed for the evolution of hydrogen and oxygen in the Dual Thin Layer Cell compared to the classical cell suggests that the vacuum also affects the local pH. In the classical cell the continuous evaporation of CO₂ shifts the equilibrium of Eq. (2) in the vicinity of the working electrode to the right hand side. This does not only reduce the local CO₂ concentration but also increases the local concentration of OH⁻. Thus, the onset potential for both hydrogen and oxygen evolution is shifted to higher values compared to an H₂/H⁺-reference electrode at bulk pH. Hence, if the electrode is deposited on the Teflon membrane as in the classical cell, CO₂ reduction proceeds under significantly different conditions than expected from the bulk composition of the electrolyte.

4. Conclusion

In this work, we studied CO₂ reduction on a gold electrode in two different DEMS cells, and introduced a new method for direct quantification of formed CO using online mass spectrometry. In the classical cell, the working electrode is directly sputter deposited on the Teflon membrane and is therefore located in the direct vicinity of the interface between vacuum and electrolyte. This changes the environment of the working electrode in two ways: the local concentration of CO₂ decreases due to its evaporation

and along with it the local pH becomes more alkaline. This results in rather low faradaic efficiencies for CO₂-reduction and in a shift of the onset potential for hydrogen evolution, CO₂ reduction and oxygen evolution. By employing the Dual Thin Layer Cell we can create a spatial separation of the working electrode and the vacuum/electrolyte interface, thus, eliminating the problems observed in the classical cell.

In order to derive quantitative information from the ionic current for mass 28 on the amounts of formed CO, it is necessary to eliminate the contribution from CO₂ fragmentation. In this work we have shown that this can be achieved by reducing the cathode potential of the ion source from -70 V to -27.5 V, thus avoiding fragmentation of CO₂ to CO⁺ during the ionization process. This method has the advantage that it comes along with a much lower noise level than matrix calibration.

Furthermore, we describe in this article a method to calibrate the Dual Thin Layer Cell for CO: We propose to use oxygen evolution in the bicarbonate containing electrolyte as an internal standard to determine the transfer efficiency of CO. After leakage calibration for CO we obtain K_{CO}^+ (28) from which we can determine together with N_{CO} the value of K_{CO}^{\ominus} (28). Knowledge of the latter allows quantification of the measured ionic currents for mass 28. The validity of the method was confirmed by the fact that we can predict the faradaic current observed during a DEMS-experiment correctly from the measured ionic currents for mass 2 and mass 28.

Author statement

CB designed the setup and conceived the experiment.

CB interpreted the data and wrote the manuscript, with input from MK.

CRediT authorship contribution statement

Christoph J. Bondue: Conceptualization, Data curation, Formal analysis, Investigation, Writing - original draft. **Marc T.M. Koper:** Conceptualization, Funding acquisition, Writing - review & editing.

Declaration of competing interest

None.

Acknowledgement

We gratefully acknowledge financial support from the Netherlands Organization for Scientific Research (NWO) and Shell Global Solutions in the framework of the Advanced Research Center Chemical Building Blocks Consortium (ARC-CBBC).

The authors want to thank Prof. Helmut Baltruschat from Bonn University and Dr. Zenonas Jusys from Ulm University for helpful discussions regarding the construction of DEMS-system.

The authors also acknowledge gratefully the Fine Mechanical Department of Leiden University and particularly Thijs Hoogenboom for ideas and technical support during the construction of the DEMS-system.

Appendix A. Supplementary data

Supplementary data to this article can be found online at <https://doi.org/10.1016/j.jelechem.2020.113842>.

References

- [1] S. Bruckenstein, R.R. Gadde, Use of a porous electrode for in situ mass spectrometric determination of volatile electrode reaction products, *J. Am. Chem. Soc.* 93 (3) (1971) 793–794.
- [2] H. Baltruschat, Differential electrochemical mass spectrometry, *J. Am. Soc. Mass Spectrom.* 15 (12) (2004) 1693–1706.
- [3] O. Wolter, J. Heitbaum, Differential electrochemical mass spectrometer (DEMS) - a NEW method for the study of electrode processes, *Ber. Bunsenges. Phys. Chem.* 88 (1984) 2–6.

- [4] P. Khanipour, M. Löffler, A.M. Reichert, F.T. Haase, K.J.J. Mayrhofer, I. Katsounaros, Electrochemical real-time mass spectrometry (EC-RTMS): monitoring electrochemical reaction products in real time, *Angew. Chem. Int. Ed.* 58 (22) (2019) 7273–7277.
- [5] H. Baltruschat, S. Ernst, Molecular adsorbates at single-crystal platinum-group metals and bimetallic surfaces, *ChemPhysChem* 12 (1) (2011) 56–69.
- [6] A.A. Abd-El-Latif, E. Mostafa, S. Huxter, G. Attard, H. Baltruschat, Electrooxidation of ethanol at polycrystalline and platinum stepped single crystals: a study by differential electrochemical mass spectrometry, *Electrochim. Acta* 55 (27) (2010) 7951–7960.
- [7] Z. Jusys, T.J. Schmidt, L. Dubau, K. Lasch, L. Jörissen, J. Garche, R.J. Behm, Activity of PtRuMeOx (Me = W, Mo or V) catalysts towards methanol oxidation and their characterization, *J. Power Sources* 105 (2) (2002) 297–304.
- [8] A. Manzo-Robledo, A.-C. Boucher, E. Pastor, N. Alonso-Vante, Electro-oxidation of carbon monoxide and methanol on carbon-supported Pt–Sn nanoparticles: a DEMS study, *Fuel Cells* 2 (2) (2002) 109–116.
- [9] S. Fierro, T. Nagel, H. Baltruschat, C. Comninellis, Investigation of the oxygen evolution reaction on Ti/IrO₂ electrodes using isotope labelling and on-line mass spectrometry, *Electrochem. Commun.* 9 (8) (2007) 1969–1974.
- [10] E.L. Clark, M.R. Singh, Y. Kwon, A.T. Bell, Differential electrochemical mass spectrometer cell design for online quantification of products produced during electrochemical reduction of CO₂, *Anal. Chem.* 87 (15) (2015) 8013–8020.
- [11] E.L. Clark, A.T. Bell, Direct observation of the local reaction environment during the electrochemical reduction of CO₂, *J. Am. Chem. Soc.* 140 (22) (2018) 7012–7020.
- [12] A. Javier, B. Chmielowiec, J. Sanabria-Chinchilla, Y.-G. Kim, J.H. Baricuatro, M.P. Soriaga, A DEMS study of the reduction of CO₂, CO, and HCHO pre-adsorbed on Cu electrodes: empirical inferences on the CO₂RR mechanism, *Electrocatalysis* 6 (2) (2015) 127–131.
- [13] D. Kolbe, W. Vielstich, Adsorbate formation during the electrochemical reduction of carbon dioxide at palladium—a DEMS study, *Electrochim. Acta* 41 (15) (1996) 2457–2460.
- [14] E.R. Cave, J.H. Montoya, K.P. Kuhl, D.N. Abram, T. Hatsukade, C. Shi, C. Hahn, J.K. Nørskov, T.F. Jaramillo, Electrochemical CO₂ reduction on Au surfaces: mechanistic aspects regarding the formation of major and minor products, *Phys. Chem. Chem. Phys.* 19 (24) (2017) 15856–15863.
- [15] O. Wolter, J. Heitbaum, The adsorption of CO on a porous Pt-electrode in sulfuric acid studied by DEMS, *Ber. Bunsenges. Phys. Chem.* 88 (1984) 6–10.
- [16] D. Tegtmeier, J. Heitbaum, A. Heindrichs, Electrochemical on line mass spectrometry on a rotating electrode inlet system, *Ber. Bunsenges. Phys. Chem.* 93 (2) (1989) 201–206.
- [17] G. Samjeské, H. Wang, T. Löffler, H. Baltruschat, CO and methanol oxidation at Pt-electrodes modified by Mo, *Electrochim. Acta* 47 (22–23) (2002) 3681–3692.
- [18] M.T. de Groot, M.T.M. Koper, The influence of nitrate concentration and acidity on the electrocatalytic reduction of nitrate on platinum, *J. Electroanal. Chem.* 562 (1) (2004) 81–94.
- [19] Z. Jusys, H. Massong, H. Baltruschat, A new approach for simultaneous DEMS and EQCM: electro-oxidation of adsorbed CO on Pt and Pt–Ru, *J. Electrochem. Soc.* 146 (3) (1998) 1093–1098.
- [20] C.J. Bondue, A.A. Abd-El-Latif, P. Hegemann, H. Baltruschat, Quantitative study for oxygen reduction and evolution in aprotic organic electrolytes at gas diffusion electrodes by DEMS, *J. Electrochem. Soc.* 162 (3) (2015) A479–A487.
- [21] R.T. Ferrell, D.M. Himmelblau, Diffusion coefficients of nitrogen and oxygen in water, *J. Chem. Eng. Data* 12 (1) (1967) 111–115.
- [22] D.L. Wise, G. Houghton, Diffusion coefficients of neon, krypton, xenon, carbon monoxide and nitric oxide in water at 10–60°C, *Chem. Eng. Sci.* 23 (10) (1968) 1211–1216.
- [23] S. Iqbal, C. Bondü, H. Baltruschat, Quantitative determination of H₂Se at model metal fcc(111) Selenide surface: DEMS, STM, and AFM studies, *J. Phys. Chem. C* 119 (35) (2015) 20515–20523.